Published in final edited form as:
CNS Neurol Disord Drug Targets. 2013 May 1; 12(3): 325–337.

HSP27 Protects the Blood-Brain Barrier Against Ischemia-Induced Loss of Integrity

Rehana K. Leak[*,1], **Lili Zhang**[*,2,3], **R. Anne Stetler**[2,3], **Zhongfang Weng**[2,3], **Peiying Li**[2,3], **G. Brandon Atkins**[4], **Yanqin Gao**[2], and **Jun Chen**[2,3,5]

[1]Division of Pharmaceutical Sciences, Duquesne University Pittsburgh, PA 15282, USA

[2] State Key Laboratory of Medical Neurobiology and Institute of Brain Sciences Fudan University, Shanghai 200032, China

[3]Center for Cerebrovascular Disease Research, University of Pittsburgh School of Medicine Pittsburgh, PA 15213, USA

[4]Case Cardiovascular Research Institute, Department of Medicine, Case Western Reserve University School of Medicine, Cleveland, OH 44106, USA

[5]Geriatric Research, Educational and Clinical Center, Veterans Affairs Pittsburgh Health Care System, Pittsburgh, PA 15261, USA

Abstract

Loss of integrity of the blood-brain barrier (BBB) in stroke victims initiates a devastating cascade of events including extravasation of blood-borne molecules, water, and inflammatory cells deep into brain parenchyma. Thus, it is important to identify mechanisms by which BBB integrity can be maintained in the face of ischemic injury in experimental stroke. We previously demonstrated that the phylogenetically conserved small heat shock protein 27 (HSP27) protects against transient middle cerebral artery occlusion (tMCAO). Here we show that HSP27 transgenic overexpression also maintains the integrity of the BBB in mice subjected to tMCAO. Extravasation of endogenous IgG antibodies and exogenous FITC-albumin into the brain following tMCAO was reduced in transgenic mice, as was total brain water content. HSP27 overexpression abolished the appearance of TUNEL-positive profiles in microvessel walls. Transgenics also exhibited less loss of microvessel proteins following tMCAO. Notably, primary endothelial cell cultures were rescued from oxygen-glucose deprivation (OGD) by lentiviral HSP27 overexpression according to four viability assays, supporting a direct effect on this cell type. Finally, HSP27 overexpression reduced the appearance of neutrophils in the brain and inhibited the secretion of five cytokines. These findings reveal a novel role for HSP27 in attenuating ischemia/reperfusion injury - the maintenance of BBB integrity. Endogenous upregulation of HSP27 after ischemia in wild-type animals may exert similar protective functions and warrants further investigation. Exogenous

For correspondence, please address: Dr. Jun Chen Department of Neurology S507 Biomedical Science Tower University of Pittsburgh Pittsburgh PA 15213 TEL: 412-648-1263 FAX: 412-648-1239 chenj2@upmc.edu or Dr. Yanqin Gao State Key Laboratory of Medical Neurobiology Fudan University Shanghai, China yqgao@shmu.edu.cn.

CONFLICT OF INTEREST

The authors declare no conflicts of interest with other individuals or organizations.

enhancement of HSP27 by rational drug design may lead to future therapies against a host of injuries, including but not limited to a harmful breach in brain vasculature.

Keywords

endothelial cell; heat shock protein; HSP25; HSPB1; microvessel; stroke; tight junction; vascular

INTRODUCTION

Heat shock proteins are highly evolutionarily conserved because of their critical importance during cellular stress. Heat shock denatures vulnerable proteins that must then be refolded or degraded for the cell to remain viable. In order to achieve these naturally protective functions, multiple heat shock proteins are rapidly synthesized by stressed cells. Of these proteins, heat shock protein 70 (HSP70) has been studied the most and found to help battle apoptosis, refold misfolded proteins, and chaperone unwanted proteins towards degradation [1, 2]. The more recently discovered HSP27 has similarly manifold functions. For example, HSP27 suppresses caspase activation [3, 4] and inhibits cytochrome c release [5, 6]. HSP27 also decreases protein aggregations [7] and favors degradation by the proteasome [8, 9]. Our recent work reveals that HSP27 overexpression can protect against ischemic injury in a robust and prolonged manner [10, 11], supporting other investigations on virally mediated HSP27 overexpression [12] and HSP27 peptide transduction [13] in experimental stroke. In addition, we demonstrated that HSP27 was activated by protein kinase D and protected the *in vivo* brain by inactivating apoptosis signal regulating kinase 1 (ASK1) [10, 11]. Although multiple mechanisms underlying the impact of HSP27 on survival have been discovered, whether HSP27 can also protect against a harmful breach in the integrity of the blood-brain barrier (BBB) is still unknown. One of the most disabling consequences of stroke is destruction of the BBB [14] and severe brain edema [15, 16]. Brain edema predicts poor neurological outcome and is thought to arise from increased BBB permeability, matrix metalloproteinases, and aquaporins [15]. Protection against these damaging sequelae of stroke may save human lives. Thus, maintenance of BBB integrity following stroke is a critical therapeutic necessity and deserves detailed investigation.

The present study investigates the impact of HSP27 on BBB permeability. Several correlative studies already indicate that HSP27 induction can parallel a breach in vascular integrity. Although this endogenous response may be a protective mechanism against vascular injury, this has not been directly tested with HSP27 overexpression or knockdown. First, aged rats suffer from greater hemorrhage-induced injury and also have higher expression of HSP27 [17, 18]. Second, a study of lung edema reported enhanced HSP27 phosphorylation [19]. Third, preconditioning with low doses of thrombin attenuates the brain edema caused by higher doses and increases HSP27 expression within astrocytes [20, 21]. Fourth, hyperthermia also induces HSP27 in brain microvasculature and may compromise BBB integrity [22]. Fifth, cerebrovascular tone has been argued to be modulated by p38 MAPK and HSP27, although HSP27 levels were not directly manipulated in this study [23]. Finally, one study used the heat shock protein inducer geldanamycin to induce HSP27 in an ischemia model and found a reduction in edema [24]. However,

geldanamycin is not specific to HSP27 as it also induces HSP70 and there is some evidence that HSP70 can reduce BBB permeability after injury. For example, systemically delivered neural precursor cells transduced with HSP70 protein can protect the BBB against ischemia and reduce the activation of matrix metalloprotease 9 [25, 26]. Others have reported that geldanamycin attenuates BBB disruption and edema following intracerebral hemorrhage, perhaps by upregulating HSP70 [27]. Despite these advances in the study of heat shock proteins and their impact on the BBB, the impact of HSP27 on BBB permeability remains to be determined. Thus, the present study tests the hypothesis that the BBB is protected by transgenic HSP27 overexpression in an experimental stroke model.

MATERIALS AND METHODS

Animals and Surgeries

All efforts were made to minimize animal suffering. Experimental protocols were approved by the University of Pittsburgh Institutional Animal Care and Use Committee and carried out in adherence with the NIH Guide for the Care and Use of Laboratory Animals. Male 3-5 month old C57/B6 mice were housed at room temperature in a 12:12 light dark cycle with *ad libitum* access to food and water. Transgenic HSP27 overexpressors were generated as described previously [10]. Briefly, the chimeric transgene contained human HSP27 cDNA under control of the cytomegalovirus enhancer and a chicken β-actin promoter within the first intron. Wild-type mice backbred from the same transgenic lines were used as controls.

For tMCAO, STAIR guidelines were followed for evaluation of stroke efficacy. The surgeon and the raters for all subsequent assays were always blinded to mouse genotype. All mice were anesthetized with 1.5% isoflurane in a 30% O_2/68.5% N_2O mixture under spontaneous breathing. Rectal temperature was maintained at 37.0 ± 0.5°C with a heating pad (CMA 150, Carnegie Medicine, Sweden). A tail cuff (XBP1000 Systems, Kent Scientific Corporation, Torrington CT) was used to monitor blood pressure. A monofilament nylon suture was inserted into external carotid for 60 min as previously described [28]. Sham animals were subjected to the same surgery with the exception of tMCAO. Only 4 wild type and 2 transgenic mice died between 24 and 72 h after tMCAO.

Regional cerebral blood flow (rCBF) was monitored by laser Doppler flowmetry (PeriFlux system 5000, Perimed, Stockholm, Sweden) as described previously [28]. In addition, the laser speckle technique was used for two-dimensional microcirculation imaging [29, 30]. Briefly, a laser diode (785 nm) illuminated the skull surface while a CCD camera (PeriCam PSI System, Perimed, Jarfalla, Sweden) was positioned above the head. Speckle contrast is defined as the ratio of the standard deviation of pixel intensity to mean pixel intensity. This measures CBF as derived from speckle visibility relative to the velocity of the light-scattering particles in blood. CBF was converted to correlation time values. These values are inversely proportional to mean blood velocity.

Neurological Score Assessments

Neurological scores were calculated with the same scoring scheme as described by Dimitrijevic and colleagues [31] - 0: no visible neurological deficits; 1, forelimb flexion; 2,

contralateral forelimb grips weakly (the rater pulls the tail gently while the animal is on a padded surface); 3, circling to the paretic side only when pulled by the tail (the animal is allowed to move freely); and 4, spontaneous circling. Thus, “0” was the best neurological score (least deficits) and “4” was the worst neurological score (greatest deficits).

Infarct Volume

At 24 h after reperfusion following tMCAO, mice were sacrificed with CO_2 and brains removed. The forebrain was sliced into seven 1 mm thick coronal sections and stained with 3% 2,3,5-triphenyltetrazolium (TTC, Sigma-Aldrich, St. Louis MO). An MCID image analysis system (Imaging Research, G.E. Healthcare Biosciences, Pittsburgh PA) was used to calculate infarct volume with and without correction for brain edema [28]. A separate cohort of animals was sacrificed at 96 h after tMCAO and perfused with saline and 4% paraformaldehyde. These brains were cryoprotected and sliced into 25 μm coronal sections for microtubule associated protein 2 (MAP2) immunofluorescent staining (see below).

BBB Disruption

For measurements of BBB permeability, extravasation of mouse IgG into brain parenchyma was assessed. Mice were perfused and brains removed. Coronal brain sections were cut at 25 μm and blocked in 5% bovine serum albumin for 1 h. Sections were immunostained with biotinylated horse anti-mouse IgG (1:500, Vector Laboratories, Burlingame, CA), followed by incubation in streptavidin/horseradish peroxidase reagents (Vectastain Elite ABC; Vector Laboratories) and then 0.5 mg/ml diaminobenzidine with 0.05% H_2O_2. Seven sections encompassing the MCA territory were quantified for cross-sectional area of IgG staining. These data were summed and multiplied by the distance between sections (1 mm) to yield volume in mm^3.

As a second measurement of BBB integrity, the blood brain transfer coefficient (*K*i) for fluorescein isothiocyanate (FITC)-albumin was measured as previously described [31]. FITC-albumin was injected into the femoral vein and arterial blood was collected at 5 min intervals for 20 min to measure FITC-albumin in plasma. Mice were then decapitated and hemispheres weighed. Brains were homogenized in 50 mmol/L Tris buffer and centrifuged at 3000 rpm for 30 min. Methanol was added to the supernatant at a ratio of 1:1 and the mixture centrifuged. The *K*i was assessed according to the equation: $Ki=(C_{br}–V_oC_{bt})/\int C_{pl}\cdot dt$, where C_{br} is the concentration of FITC-albumin in brain at decapitation (ng/g), C_{bl} is the concentration of FITC-albumin (ng/mL) in the final blood sample, V_o is regional blood volume (mL/g), and $\int C_{pl}\cdot dt$ is the integral of the arterial concentration of FITC-albumin over time t. V_o was determined in separate mice decapitated 1 minute after injection of FITC-albumin.

Brain Water Content

Brains were removed from mice following euthanasia in a CO_2 chamber and weighed both while still wet and after oven-drying (100°C) for 2 days. Water content was calculated according to the formula: (wet weight – dry weight) / wet weight × 100.

Microvessel Isolation and Western blotting

Microvessels were isolated by following previously described methods [32]. Animals were decapitated and brains immersed in cold buffer A (103 mM NaCl, 4.7 mM KC1, 2.5 mM $CaC1_2$, 1.2 mM KH_2PO_4, 1.2 mM $MgSO_4$, 15 mM HEPES, pH 7.4) and homogenized in 5-fold volumes of buffer B (103 mM NaCl, 4.7 mM KC1, 2.5 mM $CaC1_2$, 1.2 mM KH_2PO_4, 1.2 mM $MgSO_4$, 15 mM HEPES, 25 mM HCO_3, 10 mM glucose, 1 mM sodium pyruvate, and 1g/100 ml dextran, pH 7.4) using a Teflon homogenizer. An equal volume of 25% bovine serum albumin was used to suspend the homogenate, followed by centrifugation at 5800×g at 4°C for 30 min. The pellet was then resuspended in 10 ml of buffer B and pushed through an 85 μm nylon mesh. The filtrate was passed over a 3×4 cm column housing 0.4 mm glass beads. A 44 μm nylon mesh was placed at the bottom of the glass beads. Beads were then washed with 400 ml of buffer B. Only microvessels adhere to the glass beads in this preparation. The glass beads were repeatedly agitated in buffer B and the supernatant decanted and spun at 500×g for 5 min. The pellet was homogenized in 600 μL of cytoskeleton-stabilizing buffer (10 mM HEPES, pH 7.4, 250 mM sucrose, 150 mM KCl, 1 mM EGTA, 3 mM $MgCl_2$, protease inhibitor cocktail (Sigma-Aldrich), 1 mM Na_3VO_4, and 1% Triton X-100 and incubated on ice for 20 min. After centrifugation at 15,000g for 15 min at 4°C, the supernatant (Triton-soluble fraction) was probed for HSP27 (1:1000, Abcam, Cambridge MA) by standard Western blotting with enhanced chemiluminescence detection reagents (Kirkegaard & Perry Laboratories, Gaithersberg MD).

The final pellet from the above centrifugation was further resuspended in 400 μL Laemmli buffer (Bio-Rad, Hercules CA) with 1 M urea and sonicated, as described by Wacker and colleagues [33]. Samples were then supplemented with 20 μL mercaptoethanol, incubated at 95°C for 10 min and allowed to cool to room temperature, followed by a 10 min centrifugation at 15,000g. The supernatant (now the Triton-insoluble fraction) was also subjected to Western immunoblotting with the following antibodies: HSP27 (1:1000, Abcam), occludin (1:500, Invitrogen, Life Technologies, Carlsbad CA), VE-cadherin (1:500, Abcam), zonula occludens-1 (ZO-1; 1:250, Abcam), and claudin-5 (1:500, EMD Millipore, Billerica MA). The optical density of bands was quantified in Image J (NIH Image, Bethesda MD).

Immunofluorescent staining

For MAP2 staining of neurons and myeloperoxidase (MPO) staining of neutrophils, we used standard immunofluorescence with anti-MAP2 (1:200, Santa Cruz Antibodies H-300, Santa Cruz CA) and anti-MPO (1:150, Abcam). Primary antibodies were incubated at 4°C overnight followed by incubation with fluorescent secondary antibodies (1:500, Jackson ImmunoResearch, West Grove PA) for 1 h. Images were captured with a Nikon TE2000 fluorescent microscope (Nikon Instruments, Melville NY). MPO positive profiles in the MCA territory were counted in 6 random fields/section at 200× magnification on 3sections/animal.

Lectin and Terminal Deoxynucleotidyl Transferase-mediated Biotinylated dUTP Nick End Labeling (TUNEL) Staining

Cerebral vessels were identified by transcardial administration (5 min before euthanasia) of biotinylated-lycopersicon esculentum lectin (tomato lectin, 1.25 mg/kg; Vector Laboratories), which labels endothelial cells in perfused vessels, as described by Chu and colleagues [34]. Lectin staining was visualized with fluorescent streptavidin (1:1000, Vector Laboratories).

The Klenow fragment of DNA polymerase I-mediated nick end-labeling technique (a modified TUNEL) was performed to visualize apoptotic profiles as described previously [35]. Sections were incubated in a moist air chamber at 37°C for 1 h in a labeling mixture containing 10 μM each of dGTP, dCTP, and dTTP; biotinylated dATP; and 100 U/ml *E. coli* Klenow fragment (GibcoBRL, Life Technologies) in a 1× reaction buffer (50 mM Tris-HCl, pH 8.0, 10 mM $MgCl_2$, 50 mM NaCl). The biotinylated dUTP 3'-OH DNA end-label was detected by incubation for 30 min in Streptavidin-Cy3 (Sigma-Aldrich). Double-label immunofluorescence for lectin and TUNEL was visualized with confocal microscopy (Olympus Fluoview FV1000, Olympus, Center Valley PA).

Proteomic Array Analysis

The ChemiArray™ Mouse Antibody Arrays kit (Chemicon, Temecula CA) was used for proteomic cytokine analysis according to manufacturer's instructions. Blocking buffer was added to each membrane for 30 min. The membrane was then exposed to brain protein samples for 1.5 h. This was followed by washes and incubation with biotin-conjugated anti-cytokine primary antibodies for 1.5 h at room temperature. The membrane was washed again and incubated with HRP-conjugated streptavidin for 2 h. Signal was detected with a chemiluminescence imaging system and signal intensity was quantified by densitometry with MCID. For specificity validation, three pairs of positive controls and two pairs of negative controls are included with each array.

Primary Endothelial Cultures and Oxygen-Glucose Deprivation (OGD)

Primary human brain microvascular endothelial cells were purchased from Cell Systems (Cat. No. ACBRI 376 V, Kirkland WA). These endothelial cells were initiated by elutriation of dispase dissociated cortical tissue. We grew the cells in Clonetics EGM2-MV media (CC-3202, Lonza, Walkersville MD) and discarded them after passage 8.

To mimic ischemia *in vitro*, medium was replaced with glucose-free medium and cultures were placed in an airtight chamber (Billups-Rothenberg, Del Mar CA) that was flushed with 95% argon and 5% CO_2 gas for 5 min and sealed. Cells were incubated at 37°C for 120 min in these OGD conditions before returning them to 95% air and 5% CO_2.

Lentiviral HSP27 Constructs

Lentiviral vectors overexpressing rat full-length HSP27 were constructed as described previously [11]. The hemagglutinin (HA) tagged cDNA was inserted into the lentiviral transfer vector FSW under the control of phosphoglycerate kinase (PGK) promoter. A plasmid mixture containing 435 μg of pCMVΔR8.9 (packaging construct), 237 μg of

pVSVG (envelope plasmid) and 675 μg of FSW (transfer vector) was suspended in 34.2 ml of $CaCl_2$ (250 mM) and co-transfected into human kidney 293 FT cells. The supernatant was collected 72 h after transfection, filtered through a 0.45 μm filter flask and centrifuged at 21,000 rpm for 2 h using an SW28 rotor (Beckman Coulter, Indianapolis IN). Viruses were further purified by sucrose gradient ultracentrifugation.

Lentiviral transfections were performed 3 days prior to exposure to OGD as described above. Viability assays were performed 24 h after OGD (see below). Infections were visualized by fixing cells in 4% paraformaldehyde, staining with anti-HA (1:500, Santa Cruz Biotechnology CA), anti-cleaved caspase-3 (Asp175) rabbit monoclonal antibody (1:200, Cell Signaling, MA), and the DAPI counterstain. Additionally, Western immunoblotting was used to ensure expression of HSP27 and the HA tag in infected lysates with antibodies against HSP27 (1:1000, Abcam) and HA (1:1000, Santa Cruz Biotechnology) as described above.

Endothelial Cell Viability Assays

Viability was assessed using the 3-(4,5-Dimethylthiazol-2-yl)-2,5-diphenyltetrazolium bromide (MTT) assay for mitochondrial activity and the lactate dehydrogenase assay (LDH, Sigma-Aldrich) for loss of membrane integrity. Cells were treated with 0.5 mg/ml MTT for 1 h at 37°C, followed by addition of 100 μL dimethyl sulfoxide. Absorbance was measured at 570 nm over the course of 5 min. The LDH assay was performed according to manufacturer's instructions.

Tetramethylrhodamine Methyl Ester (TMRM) Fluorescent Assay

TMRM was used as a cationic, mitochondrial selective probe for the mitochondrial membrane potential deltapsi. The mitochondrial membrane potential MitoPT™ kit (AbD Serotec, Raleigh NC) was used according to manufacturer's instructions. TMRM accumulates only in mitochondria and signal falls when deltapsi collapses. Fluorescence was measured on a plate reader at excitation 510-560 nm and emission 570-620 nm.

Caspase-3 Activity Assay

Caspase-3-like activity was measured using fluorogenic substrates *Ac*-DEVD-*AFC*, as described previously [36, 37]. Briefly, 100 μg of extracted protein was incubated for 1 h at 37°C with a buffer containing 25 mmol/L HEPES (pH 7.5), 10% sucrose, 0.1% 3-[(3-cholamidopropyl) dimethylammonio]-1-propane sulfonate, 5-mmol/L chlorophenothane, and 5-mmol/L edetic acid in 150 μL and with 25-mol/L fluorogenic peptide cleavage substrate (Medical & Biological Laboratories, Watertown MA). Parallel protein extracts were also incubated in reaction buffer with 5 μmol/L of caspase inhibitor DEVD-CHO for 30 min prior to the addition of assay substrates. These values were subtracted from those obtained without the inhibitor.

Statistical Analyses

Data are expressed as the mean and S.E.M. and were analyzed by ANOVA followed by *post hoc* Bonferroni/Dunn tests. The difference in means between 2 groups was assessed by the

two-tailed *t* test. For *in vitro* primary endothelial cultures, data are presented as the average of at least 3 independent experiments. Differences were deemed significant at $p \leq 0.05$.

RESULTS

Our findings support the hypothesis that HSP27 protects the BBB from ischemia/reperfusion injury. Transgenic animals exhibited reduced extravasation of water, blood-borne molecules, and inflammatory cells into brain parenchyma. Microvessel proteins were protected from ischemic injury and apoptosis in cells along microvessel walls was almost completely abolished in transgenics. HSP27 also protected primary endothelial cells from an *in vitro* model of ischemia. Finally, the release of several inflammatory cytokines was ameliorated by HSP27 overexpression. As a whole, the present findings thus suggest a new role for the small HSP27 stress protein.

Reduction in Infarct Volume and Behavioral Deficits

In order to verify that HSP27 is protective against ischemic injury, infarct volumes were measured following induction of tMCAO in wild-type and HSP27 overexpressors. Animals were sacrificed at 24 h and 96 h after tMCAO and brain sections were stained with TTC (24 h group) and the neuronal phenotypic marker MAP2 (96 h group). These two independent assays revealed a significantly smaller infarct size in transgenic mice at both timepoints (Figure 1A). Measurements of the region of loss of TTC and MAP2 staining are illustrated in Figure 1B. This is a direct measurement of infarct volume and may be subject to edema and swelling in the affected zone. Figure 1C illustrates an indirect measurement of infarct volume that is less subject to the impact of edema and swelling because it reports the size of healthy, TTC and MAP2-positive regions in the ipsilateral hemisphere subtracted from the total size of the contralateral hemisphere. This latter indirect measurement reduces the impact of brain swelling and edema on volumetric measurements because the majority of swelling occurs in MAP2 and TTC-negative zones. Both direct and indirect types of quantification replicate our previous findings that HSP27 reduces infarct volume after tMCAO [10, 11].

Transgene expression might be argued to affect the vascular system so that transgenics may not receive the same ischemic injury as control mice. In order to ensure that the reduction in infarct volume was not confounded by alterations in blood flow, we measured rCBF by laser Doppler 15 min and 45 min following initiation of tMCAO and 15 min after reperfusion (Figure 1D). No difference in blood flow was detected, suggesting that both groups were indeed exposed to the same insult. This was also supported by directly measuring the ischemic area with two-dimensional laser speckle (Figure 1E). Again, no difference between transgenics and wild-type animals could be detected either in the ischemic core or penumbra. Thus, the protection against tMCAO in transgenic animals was not likely to result from differences in the initial ischemic stimulus *per se*.

We have previously shown that HSP27 reduces the behavioral deficits elicited by tMCAO [10, 11]. In those studies, transgenics performed better on the Rotarod, foot fault, and Morris water maze tests. In the present study, we calculated neurological scores. At both 1 and 4 days after tMCAO, protection against neurological deficits was apparent in transgenics

(Figure 1F). Notably, the protection was more striking at day 4, supporting the notion that the effect was not going to wane over time.

Impact on BBB permeability and Brain Water Content

Following the verification of HSP27-induced protection, we tested the hypothesis that BBB permeability was reduced in transgenics exposed to tMCAO. First, we measured IgG extravasation into brain parenchyma by directly staining for mouse IgG immunoreactivity (Figure 2A). The surface areas of IgG infiltration from 7 sections are summed to reveal total IgG-staining volume in Figure 2B. Individual surface areas of IgG staining in each of the 7 coronal sections are also illustrated to capture the rostrocaudal extent of vascular protection (Figure 2C). Both types of data reveal a significant reduction in IgG extravasation into brain parenchyma in transgenics.

As a second means of quantifying loss of BBB integrity we perfused animals with FITC-albumin. As expected from the IgG staining results, tMCAO increased the entry of FITC fluorescence into the brain in both wild-type and transgenic groups. However, transgenics had lower extravasation of FITC-albumin in both the cortex and the striatum at 24 and 96 h post-ischemic injury (Figure 2D). These IgG staining and FITC-albumin results indicate that the BBB is less compromised by ischemic injury in transgenics.

Another consequence of BBB disruption after ischemia is severe brain edema. Thus, brain water content was measured by weighing brains before and after a drying period. As expected, brain water content was lessened in the transgenics at both 24 h and 96 h (Figure 2E). These findings suggest that HSP27 also protects against water influx into the brain.

Protection of Microvessel Integrity

Although HSP27 is predominantly an astrocytic protein, our previous studies revealed transgenic overexpression of HSP27 in neurons, astrocytes, and microvessels [10, 11]. In order to further confirm HSP27 transgene expression in microvessels, we isolated microvessels for immunoblotting. By definition, HSP27 is a stress-responsive protein, similar to all other heat shock proteins [38]. Thus, one might expect tMCAO to raise HSP27 levels as an endogenous protective response. As expected, tMCAO raised HSP27 levels in wild-type mice (Figure 3A). HSP27 was already basally high in microvessels of transgenics and tMCAO did not raise levels beyond this. Even without an additional rise, HSP27 expression in transgenics was higher than in wild-type animals under tMCAO conditions.

In order to assess damage to microvessels, we measured levels of four proteins normally expressed in microvessels. With disruption of the BBB, these proteins can become insoluble and/or degraded. We found that occludin, ZO-1, VE-cadherin were all reduced 24 h following ischemia in wild-type animals in both the Triton-X insoluble (Figure 3B, C) and soluble (data not shown) fractions. There was no impact of tMCAO on claudin-5. Notably, transgenics exhibited less loss of microvessel proteins than wild-type controls.

In order to further examine microvessel integrity *in situ*, we perfused animals with a fluorescent lectin and stained sections for TUNEL-positive profiles. We noted an increase in TUNEL-positive, presumably apoptotic profiles 24 h after tMCAO both along microvessel

walls and in nearby brain parenchyma (Figure 3D). However, HSP27 brains exhibited far fewer TUNEL-positive profiles along microvessel walls in response to tMCAO (Figure 3E). Taken together, these immunoblotting and histological studies support the hypothesis that HSP27 reduces the impact of tMCAO on microvessel proteins and abolishes the rise in apoptosis in microvessel cells.

Lentiviral HSP27 Overexpression Directly Protects Primary Endothelial Cell Cultures

Primary endothelial cell cultures yield a homogenous model of capillary wall cells and are a powerful means of assaying the impact of treatments specifically on this cell population. We tested the hypothesis that infection of these cultures with a lentivirus bearing the HSP27 gene would protect endothelial cells against OGD *in vitro*. Figure 4A illustrates that many endothelial cells in these cultures were successfully infected and expressed GFP or the HA tag. Furthermore, both HSP27 protein and the HA tag were highly expressed in lenti-HSP27 infected cultures in immunoblotting experiments (Figure 4B). Primary endothelial cultures infected with lenti-HSP27 also exhibited less nuclear condensation and expressed less activated (cleaved) caspase 3 in response to OGD than cultures infected with the control lentiviral vector (Figure 4C). Cell viability was measured by the MTT (Figure 4D) and LDH assays (Figure 4E). Both assays revealed a loss in viability with OGD that was not affected by the control lentiviral construct. In contrast, lenti-HSP27 attenuated the loss in cell viability according to both measures. As another indicator of cellular health status, mitochondrial membrane potential was measured with TMRM fluorescence (Figure 4F). As expected from the MTT and LDH data, HSP27 also rescued endothelial cells from collapse of the mitochondrial membrane potential. As a final approximation of cell death pathway activation, caspase-3 activity was measured (Figure 4G). As expected from the immunofluorescence data in Figure 4C, HSP27 overexpression blunted the rise in caspase-3 activity following OGD. Taken as a unit, these multiple independent assays strongly suggest that endothelial cells are protected from ischemic cell death when they express more HSP27 protein.

Blunting of the Inflammatory Response

Ischemic injury and BBB disruption are typically accompanied by neutrophil invasion of brain parenchyma. To visualize this entry, we stained brains for MPO, a neutrophil marker (Figure 5A). tMCAO increased the number of MPO-positive cells in wild-type animals at both 24 h and 96 h (Figure 5B). However, HSP27 overexpressors exhibited far fewer MPO-positive profiles. Western immunoblotting for MPO protein was also used to assess neutrophil brain invasion (Figure 5C). As expected from the immunohistochemical findings, tMCAO greatly increased MPO protein levels and HSP27 reduced this effect. These findings support the hypothesis that HSP27 reduces the invasion of blood-borne cells into brain parenchyma.

The brain produces cytokines during ischemic injury [39, 40]. These cytokines may recruit neutrophils from the blood. Neutrophil invasion is typically accompanied by additional release of cytokines. Because neutrophil invasion following tMCAO appeared to be reduced in transgenics, we tested the hypothesis that were would also be fewer cytokines in HSP27 overexpressors. Protein arrays for 32 cytokines revealed that levels of soluble tumor necrosis

factor receptor 1 (sTFNR1), granulocyte colony stimulating factor (GCSF), tissue inhibitor of metalloproteinases 1 (TIMP1), interleukin-6 (IL-6) and monocyte chemoattractant protein 1 (MCP-1) in the tMCAO brain were all reduced by HSP27. KC (melanoma growth-stimulating activity gene) levels were not significantly impacted. These findings suggest that the reduced infiltration of blood-borne cells into the transgenic brain is accompanied by a reduction in inflammatory cytokine release.

DISCUSSION

The present study expands the protective roles of HSP27 to include maintenance of BBB integrity. Although many mechanisms underlying the protection afforded by HSP27 have been identified, the present study is the first demonstration of less extravasation of blood-borne molecules and cells into brain parenchyma in HSP27 overexpressors and a concomitant reduction of water entry into brain tissue. The impact of ischemia on loss of microvessel proteins was also ameliorated in transgenics and apoptotic cell death in microvessel walls was almost completely abolished. A direct protective effect of HSP27 on endothelial cells was confirmed in primary endothelial cultures by four independent measures. Finally, neutrophil invasion into the cortex was inhibited by transgene expression, as was the production of inflammatory cytokines. Taken together, these data argue in favor of a new mechanism of action of HSP27 - protection of the BBB - in addition to its other protective roles. Whether the impact of HSP27 on the BBB is a direct effect on endothelial cells *in vivo* remains to be verified, as our study does not preclude an indirect effect on microvessels through HSP27 overexpression in neighboring astrocytes and neurons [10, 11]. Nonetheless, the results of these studies argue in strong favor of a protective role of HSP27 against BBB damage. In light of the importance of an intact BBB in preventing stroke complications [16, 41], future studies on the mechanism through with HSP27 maintains endothelial cell structure are warranted, as are pharmacological studies targeting HSP27 with rational drug design.

We first verified that HSP27 overexpressors were indeed protected against the tMCAO model of stroke. Infarct volume and neurological deficits were both reduced in transgenics, as shown by us previously [10, 11]. Others have similarly noted that HSP27 overexpressors are protected against cardiac ischemia/reperfusion [42]. These changes occurred in the absence of changes to rCBF, so that the initial ischemic insult was comparable to wild-type animals. The present findings are consistent with our previous studies showing no difference in vasculature by injections of India ink/gelatin into wild-type and HSP27 overexpressors [10, 11]. Second, we showed that loss of BBB integrity following tMCAO was higher in wild-type animals, as suggested by greater IgG and FITC-albumin extravasation into the brain. Not surprisingly, the wet/dry weights of wild-type and transgenic brains both 24 and 96 h following tMCAO also suggested greater water entry into the wild-type brain. Consistent with each of these findings, three microvessel proteins, occludin, ZO-1, and VE-cadherin were more severely reduced in wild-type mice subjected to tMCAO. In support of this, transgene expression also almost completely abolished TUNEL-positive cell death along microvessel walls. Whether the TUNEL-positive cells are endothelial cells, pericytes, or astrocytes closely associated with the vessel wall remains to be determined. However, the cells appeared to be located inside the lectin-stained capillaries by confocal microscopy and

not next to the vessels, supporting the hypothesis they were endothelial in nature. In addition, a direct impact of HSP27 overexpression on cultured endothelial cells subjected to OGD was confirmed by assays for the reduction of MTT, LDH release from damaged, permeable membranes, loss of mitochondrial membrane potential, and the activity of caspase 3. All four assays confirmed that HSP27 protected endothelial cells against OGD injury. The present report is thus the first demonstration of a direct protective effect of HSP27 within this specific cell type.

The precise mechanism of action of HSP27 in maintaining BBB integrity was not explored in the present investigation, but may involve several layers of control, including cytoskeletal stabilization and mitochondrial quality control. As mentioned in the introduction, HSP27 can battle the recruitment of mitochondrial apoptotic factors, prevent aggregation of misfolded proteins, and enhance proteasomal degradation. For example, HSP27 appears to interfere with cell death pathways [43]. HSP27 inhibits Bax translocation to mitochondria, thereby reducing release of cytochrome c and apoptosis-inducing factor [5, 6, 44]. Consistent with these findings, HSP27 reduced caspase activity in primary endothelial cells in response to OGD in the present study and protected against mitochondrial membrane depolarization. Other mechanisms for its protective effects may include stabilization and activation of the pro-survival kinase Akt [45, 46] or inactivation of pro-apoptotic JNK signaling [47]. We previously identified a novel role for HSP27 in inactivating the kinase domain of ASK1 [10]. The inhibition of ASK1 suppressed downstream JNK activation. In further investigations we found that phosphorylation of HSP27 by protein kinase D inhibited ASK1 signaling [11].

Another mechanism underlying the protective effects of HSP27 may include stabilization of the cytoskeleton. Stabilization of the cytoskeleton by HSP27 may occur through a chaperone function [42], as HSP27 is thought to prevent the formation of insoluble actin aggregates [48, 49]. Notably, HSP27 is located in lamellipodia, filopodia, and growth cones in neurites of cultured dorsal root ganglion cells, where actin filaments are enriched [50]. As a cytoskeleton regulator, HSP27 appears to be fundamental for intracellular trafficking during mitophagy [51]. Furthermore, disruption of HSP27 causes mitochondrial fragmentation, dysfunctional mitochondrial respiration, and loss of ATP synthesis [52]. HSP27 also prevents amyloid-beta peptide induced alterations in mitochondrial size [53]. In support of these findings, the present study also showed protection of metabolic activity of primary endothelial cells by the MTT assay and prevention of mitochondrial depolarization, suggesting better overall mitochondrial health. Whether the effects of HSP27 on endothelial mitochondria are indirect or direct is not currently known and should be the subject of future investigations. In this respect it is notable that HSP27 associates with the mitochondrial fraction under conditions of thermotolerance [54]. Taken together, the literature reveals a fundamental impact of HSP27 on mitochondrial quality control and stabilization of the cytoskeleton. Furthermore, the inhibition of cell death signaling pathways by HSP27 is likely to occur both upstream and downstream of the mitochondrion and suggests multilayered regulation of cellular survival.

Cytokine expression is thought to correlate with ischemic injury and in some cases, exacerbates ongoing cell death [39, 40]. Chemokines attract neutrophils and monocytes from

the blood into the site of tissue injury. The entry of leukocytes into the brain can be enhanced if the BBB is no longer intact at the site of injury; invading leukocytes might then release greater numbers of inflammatory mediators, resulting in a vicious cycle of chronic inflammation [55, 56]. Our data reveal a significant recruitment of MPO-positive neutrophils in wild-type mice; this invasion was ameliorated in transgenics. Not surprisingly, the central invasion of neutrophils was accompanied by significant increases in levels of 5 cytokines. Again, transgene expression reduced these inflammatory responses. Cytokines such as MCP-1, which we also measured, have been shown to disrupt the BBB, perhaps by reducing tight junction integrity [31, 57]. It remains to be determined whether HSP27 protects the BBB through the reduction in cytokines or, alternatively, whether reduced cytokine release is the consequence of reduced BBB permeability and less neutrophil invasion. Both scenarios of inflammation and BBB disruption may also coexist in wild-type animals and propel each other in a cyclical fashion, as is typical of inflammatory responses during severe injuries such as stroke.

The present report suggests that drugs that induce HSP27 may ameliorate BBB damage and should be investigated as potential treatments for stroke and perhaps even intracerebral hemorrhage. Compounds that induce HSP27 often also induce HSP70 and other classes of heat shock proteins (for example, see [24]). As mentioned earlier, HSP70 battles cell death [1, 2] and there is some evidence that it may also protect the BBB from ischemia [25-27]. Indeed, heat shock itself helps preserve tight junction proteins in the BBB following osmotic stress [58]. Thus, simultaneous HSP27 and HSP70 induction may yield synergistic effects on neuroprotection and be highly desirable in the clinic. As heat shock proteins are all endogenously responsive to stress and often co-induced, potential synergy between them certainly deserves further study. Finally, given the protective roles of HSP27 in the brain, it is noteworthy that ischemia raises HSP27 levels on its own in this and other studies [59-61]. Interestingly, ischemia did not elicit this robust response in microvessels isolated from HSP27 transgenics. This lack of a stress response may be attributed to already high HSP27 levels in overexpressors so that there was no need for further induction. Furthermore, perhaps there was less stress-induced HSP27 in transgenics because the toxic impact of ischemia was reduced. The endogenous rise in HSP27 levels in wild-type animals following ischemic injury can be speculated to represent a natural attempt at self-protection of the BBB. Future studies inhibiting HSP27 under MCAO conditions are warranted to test the novel hypothesis that BBB damage would be exacerbated in its absence.

CONCLUSION

The present study reports a new protective role for HSP27 - the maintenance of BBB integrity in the face of ischemia/reperfusion injury. Apoptosis in microvessel walls was nearly abolished and microvessel proteins were less affected in HSP27 overexpressors. Extravasation of IgG antibodies and FITC-albumin into the brain was ameliorated, suggesting that the BBB was less disrupted in transgenics. Neutrophil invasion and inflammatory cytokine release were also dampened in transgenics. These inflammatory effects may be secondary to BBB protection and perhaps also further enhance BBB permeability. Primary endothelial cultures were rescued from OGD by HSP27, suggesting a direct protective effect on this important cell type. These data all point towards the potential

therapeutic value of HSP27 enhancement in the clinic. Future investigations of pharmacological inducers and/or activators of this small heat shock protein to protect against vascular damage and edema are highly warranted, given the detrimental impact of BBB disruption in human stroke victims.

Acknowledgments

*RKL and LZ contributed equally to this work. RKL, LZ, RAS, ZW, and PL performed the experiments and analyzed the data. RKL wrote the manuscript. JC and YG designed the experiments, analyzed the data, and helped write the manuscript. GBA contributed new research reagents. The authors acknowledge the administrative assistance of Pat Strickler, Deb Wilson, Mary Caruso, and Jackie Farrer. RKL was supported by a startup from the Mylan School of Pharmacy at Duquesne University. JC was supported by VA Merit Review grant and National Institutes of Neurological Disorders and Stroke grants NS043802, NS045048, NS036736, and NS056118. YG was supported by Chinese Natural Science Foundation grants 30670642, 30870794, and 81020108021. JC is a recipient of the VA Research Career Scientist Award and the RK Mellon Endowed Chair from UPMC.

LIST OF ABBREVIATIONS

ASK1	apoptosis signal regulating kinase 1
BBB	blood-brain barrier
FITC	fluorescein isothiocyanate
HSP27	heat shock protein 27
HSP70	heat shock protein 70
LDH	lactate dehydrogenase
MPO	myeloperoxidase
OGD	oxygen glucose deprivation
rCBF	regional cerebral blood flow
tMCAO	transient middle cerebral artery occlusion
TMRM	tetramethylrhodamine methyl ester
TTC	2,3,5-triphenyltetrazolium
TUNEL	terminal deoxynucleotidyl transferase-mediated biotinylated dUTP nick end labeling

REFERENCES

1. Lanneau D, Wettstein G, Bonniaud P, Garrido C. Heat shock proteins: cell protection through protein triage. Scientific World Journal. 2010; 10:1543–1552. [PubMed: 20694452]
2. Young JC. Mechanisms of the Hsp70 chaperone system. Biochem. Cell Biol. 2010; 88(2):291–300. [PubMed: 20453930]
3. Garrido C, Bruey JM, Fromentin A, Hammann A, Arrigo AP, Solary E. HSP27 inhibits cytochrome c-dependent activation of procaspase-9. FASEB. 1999; 13(14):2061–2070.
4. Voss OH, Batra S, Kolattukudy SJ, Gonzalez-Mejia ME, Smith JB, Doseff AI. Binding of caspase-3 prodomain to heat shock protein 27 regulates monocyte apoptosis by inhibiting caspase-3 proteolytic activation. J. Biol. Chem. 2007; 282(34):25088–25099. [PubMed: 17597071]

5. Bruey JM, Ducasse C, Bonniaud P, Ravagnan L, Susin SA, Diaz-Latoud C, Gurbuxani S, Arrigo AP, Kroemer G, Solary E, Garrido C. Hsp27 negatively regulates cell death by interacting with cytochrome c. Nat. Cell Biol. 2000; 2(9):645–652. [PubMed: 10980706]
6. Paul C, Manero F, Gonin S, Kretz-Remy C, Virot S, Arrigo AP. Hsp27 as a negative regulator of cytochrome C release. Mol. Cell. Biol. 2002; 22(3):816–834. [PubMed: 11784858]
7. Jakob U, Gaestel M, Engel K, Buchner J. Small heat shock proteins are molecular chaperones. J. Biol. Chem. 1993; 268(3):1517–1520. [PubMed: 8093612]
8. Parcellier A, Schmitt E, Gurbuxani S, Seigneurin-Berny D, Pance A, Chantome A, Plenchette S, Khochbin S, Solary E, Garrido C. HSP27 is a ubiquitin-binding protein involved in I-kappaBalpha proteasomal degradation. Mol. Cell. Biol. 2003; 23(16):5790–5802. [PubMed: 12897149]
9. Hohfeld J, Cyr DM, Patterson C. From the cradle to the grave: molecular chaperones that may choose between folding and degradation. EMBO. 2001; 2(10):885–890.
10. Stetler RA, Cao G, Gao Y, Zhang F, Wang S, Weng Z, Vosler P, Zhang L, Signore A, Graham SH, Chen J. Hsp27 protects against ischemic brain injury via attenuation of a novel stress-response cascade upstream of mitochondrial cell death signaling. J. Neurosci. 2008; 28(49):13038–13055. [PubMed: 19052195]
11. Stetler RA, Gao Y, Zhang L, Weng Z, Zhang F, Hu X, Wang S, Vosler P, Cao G, Sun D, Graham SH, Chen J. Phosphorylation of HSP27 by protein kinase D is essential for mediating neuroprotection against ischemic neuronal injury. J. Neurosci. 2012; 32(8):2667–2682. [PubMed: 22357851]
12. Badin RA, Lythgoe MF, van der Weerd L, Thomas DL, Gadian DG, Latchman DS. Neuroprotective effects of virally delivered HSPs in experimental stroke. J. Cereb. Blood Flow Metabol. 2006; 26(3):371–381.
13. An JJ, Lee YP, Kim SY, Lee SH, Lee MJ, Jeong MS, Kim DW, Jang SH, Yoo KY, Won MH, Kang TC, Kwon OS, Cho SW, Lee KS, Park J, Eum WS, Choi SY. Transduced human PEP-1-heat shock protein 27 efficiently protects against brain ischemic insult. FEBS. 2008; 275(6):1296–1308.
14. Platten M, Wick W. Vinken PJ, Bruyn GW. Blood-brain barrier and brain edema. Handbook of clinical neurology. 2012; 104:53–62. [PubMed: 22230435]
15. Xiao F. Bench to bedside: brain edema and cerebral resuscitation: the present and future. Acad. Emer. Med. 2002; 9(9):933–946.
16. Balami JS, Buchan AM. Complications of intracerebral haemorrhage. Lancet. 2012; 11(1):101–118.
17. Gong Y, Xi GH, Keep RF, Hoff JT, Hua Y. Aging enhances intracerebral hemorrhage-induced brain injury in rats. Acta Neurochirurgica. Supplement. 2005; 95:425–427. [PubMed: 16463895]
18. Gong Y, Hua Y, Keep RF, Hoff JT, Xi G. Intracerebral hemorrhage: effects of aging on brain edema and neurological deficits. Stroke. 2004; 35(11):2571–2575. [PubMed: 15472083]
19. Hirano S, Rees RS, Yancy SL, Welsh MJ, Remick DG, Yamada T, Hata J, Gilmont RR. Endothelial barrier dysfunction caused by LPS correlates with phosphorylation of HSP27 in vivo. Cell Biol. Toxicol. 2004; 20(1):1–14. [PubMed: 15119843]
20. Xi G, Keep RF, Hua Y, Hoff JT. Thrombin preconditioning, heat shock proteins and thrombin-induced brain edema. Acta Neurochirurgica. Supplement. 2000; 76:511–515. [PubMed: 11450080]
21. Xi G, Keep RF, Hua Y, Xiang J, Hoff JT. Attenuation of thrombin-induced brain edema by cerebral thrombin preconditioning. Stroke. 1999; 30(6):1247–1255. [PubMed: 10356108]
22. Bechtold DA, Brown IR. Induction of Hsp27 and Hsp32 stress proteins and vimentin in glial cells of the rat hippocampus following hyperthermia. Neurochem. Res. 2003; 28(8):1163–1173. [PubMed: 12834255]
23. Tong XK, Hamel E. Transforming growth factor-beta 1 impairs endothelin-1-mediated contraction of brain vessels by inducing mitogen-activated protein (MAP) kinase phosphatase-1 and inhibiting p38 MAP kinase. Mol. Pharmacol. 2007; 72(6):1476–1483. [PubMed: 17848599]
24. Lu A, Ran R, Parmentier-Batteur S, Nee A, Sharp FR. Geldanamycin induces heat shock proteins in brain and protects against focal cerebral ischemia. J. Neurochem. 2002; 81(2):355–364. [PubMed: 12064483]

25. Doeppner TR, Ewert TA, Tonges L, Herz J, Zechariah A, ElAli A, Ludwig AK, Giebel B, Nagel F, Dietz GP, Weise J, Hermann DM, Bahr M. Transduction of neural precursor cells with TAT-heat shock protein 70 chaperone: therapeutic potential against ischemic stroke after intrastriatal and systemic transplantation. Stem Cells. 2012; 30(6):1297–1310. [PubMed: 22593021]
26. Doeppner TR, Nagel F, Dietz GP, Weise J, Tonges L, Schwarting S, Bahr M. TAT-Hsp70-mediated neuroprotection and increased survival of neuronal precursor cells after focal cerebral ischemia in mice. J. Cereb. Blood Flow Metab. 2009; 29(6):1187–1196. [PubMed: 19384335]
27. Manaenko A, Fathali N, Chen H, Suzuki H, Williams S, Zhang JH, Tang J. Heat shock protein 70 upregulation by geldanamycin reduces brain injury in a mouse model of intracerebral hemorrhage. Neurochem. Int. 2010; 57(7):844–850. [PubMed: 20849898]
28. Cao G, Pei W, Ge H, Liang Q, Luo Y, Sharp FR, Lu A, Ran R, Graham SH, Chen J. In Vivo Delivery of a Bcl-xL Fusion Protein Containing the TAT Protein Transduction Domain Protects against Ischemic Brain Injury and Neuronal Apoptosis. J. Neurosci. 2002; 22(13):5423–5431. [PubMed: 12097494]
29. Ayata C, Dunn AK, Gursoy OY, Huang Z, Boas DA, Moskowitz MA. Laser speckle flowmetry for the study of cerebrovascular physiology in normal and ischemic mouse cortex. J. Cereb. Blood Flow Metab. 2004; 24(7):744–755. [PubMed: 15241182]
30. Boas DA, Dunn AK. Laser speckle contrast imaging in biomedical optics. J. Biomed. Optics. 2010; 15(1):011109.
31. Dimitrijevic OB, Stamatovic SM, Keep RF, Andjelkovic AV. Absence of the chemokine receptor CCR2 protects against cerebral ischemia/reperfusion injury in mice. Stroke. 2007; 38(4):1345–1353. [PubMed: 17332467]
32. Yin KJ, Deng Z, Hamblin M, Xiang Y, Huang H, Zhang J, Jiang X, Wang Y, Chen YE. Peroxisome proliferator-activated receptor delta regulation of miR-15a in ischemia-induced cerebral vascular endothelial injury. J. Neurosci. 2010; 30(18):6398–6408. [PubMed: 20445066]
33. Wacker BK, Freie AB, Perfater JL, Gidday JM. Junctional protein regulation by sphingosine kinase 2 contributes to blood-brain barrier protection in hypoxic preconditioning-induced cerebral ischemic tolerance. J. Cereb. Blood Flow Metab. 2012; 32(6):1014–1023. [PubMed: 22314269]
34. Chu M, Hu X, Lu S, Gan Y, Li P, Guo Y, Zhang J, Chen J, Gao Y. Focal cerebral ischemia activates neurovascular restorative dynamics in mouse brain. Frontiers Biosci. 2012; 4:1926–1936.
35. Jin K, Chen J, Nagayama T, Chen M, Sinclair J, Graham SH, Simon RP. In situ detection of neuronal DNA strand breaks using the Klenow fragment of DNA polymerase I reveals different mechanisms of neuron death after global cerebral ischemia. J. Neurochem. 1999; 72(3):1204–1214. [PubMed: 10037493]
36. Cao G, Luo Y, Nagayama T, Pei W, Stetler RA, Graham SH, Chen J. Cloning and characterization of rat caspase-9: implications for a role in mediating caspase-3 activation and hippocampal cell death after transient cerebral ischemia. J. Cereb. Blood Flow Metab. 2002; 22(5):534–546. [PubMed: 11973426]
37. Cao G, Minami M, Pei W, Yan C, Chen D, O'Horo C, Graham SH, Chen J. Intracellular Bax translocation after transient cerebral ischemia: implications for a role of the mitochondrial apoptotic signaling pathway in ischemic neuronal death. J. Cereb. Blood Flow Metab. 2001; 21(4): 321–333. [PubMed: 11323518]
38. Stetler RA, Gao Y, Signore AP, Cao G, Chen J. HSP27: mechanisms of cellular protection against neuronal injury. Curr. Mol. Med. 2009; 9(7):863–872. [PubMed: 19860665]
39. Kim JS, Gautam SC, Chopp M, Zaloga C, Jones ML, Ward PA, Welch KM. Expression of monocyte chemoattractant protein-1 and macrophage inflammatory protein-1 after focal cerebral ischemia in the rat. J. Neuroimmunol. 1995; 56(2):127–134. [PubMed: 7860708]
40. Losy J, Zaremba J. Monocyte chemoattractant protein-1 is increased in the cerebrospinal fluid of patients with ischemic stroke. Stroke. 2001; 32(11):2695–2696. [PubMed: 11692036]
41. Borgens RB, Liu-Snyder P. Understanding secondary injury. Quarterly Rev. Biol. 2012; 87(2):89–127.
42. Hollander JM, Martin JL, Belke DD, Scott BT, Swanson E, Krishnamoorthy V, Dillmann WH. Overexpression of wild-type heat shock protein 27 and a nonphosphorylatable heat shock protein

27 mutant protects against ischemia/reperfusion injury in a transgenic mouse model. Circulation. 2004; 110(23):3544–3552. [PubMed: 15569832]

43. Benn SC, Perrelet D, Kato AC, Scholz J, Decosterd I, Mannion RJ, Bakowska JC, Woolf CJ. Hsp27 upregulation and phosphorylation is required for injured sensory and motor neuron survival. Neuron. 2002; 36(1):45–56. [PubMed: 12367505]
44. Havasi A, Li Z, Wang Z, Martin JL, Botla V, Ruchalski K, Schwartz JH, Borkan SC. Hsp27 inhibits Bax activation and apoptosis via a phosphatidylinositol 3-kinase-dependent mechanism. J. Biol. Chem. 2008; 283(18):12305–12313. [PubMed: 18299320]
45. Rane MJ, Pan Y, Singh S, Powell DW, Wu R, Cummins T, Chen Q, McLeish KR, Klein JB. Heat shock protein 27 controls apoptosis by regulating Akt activation. J. Biol. Chem. 2003; 278(30): 27828–27835. [PubMed: 12740362]
46. Konishi H, Matsuzaki H, Tanaka M, Takemura Y, Kuroda S, Ono Y, Kikkawa U. Activation of protein kinase B (Akt/RAC-protein kinase) by cellular stress and its association with heat shock protein Hsp27. FEBS Lett. 1997; 410(2-3):493–498. [PubMed: 9237690]
47. Schepers H, Geugien M, van der Toorn M, Bryantsev AL, Kampinga HH, Eggen BJ, Vellenga E. HSP27 protects AML cells against VP-16-induced apoptosis through modulation of p38 and c-Jun. Exp. Hematol. 2005; 33(6):660–670. [PubMed: 15911090]
48. Panasenko OO, Kim MV, Marston SB, Gusev NB. Interaction of the small heat shock protein with molecular mass 25 kDa (hsp25) with actin. Eur. J. Biochem / FEBS. 2003; 270(5):892–901.
49. Pivovarova AV, Chebotareva NA, Chernik IS, Gusev NB, Levitsky DI. Small heat shock protein Hsp27 prevents heat-induced aggregation of F-actin by forming soluble complexes with denatured actin. FEBS. 2007; 274(22):5937–5948.
50. Williams KL, Rahimtula M, Mearow KM. Hsp27 and axonal growth in adult sensory neurons in vitro. BMC Neurosci. 2005; 6:24. [PubMed: 15819993]
51. Kang R, Livesey KM, Zeh HJ 3rd, Lotze MT, Tang D. Metabolic regulation by HMGB1-mediated autophagy and mitophagy. Autophagy. 2011; 7(10):1256–1258. [PubMed: 21691146]
52. Tang D, Kang R, Livesey KM, Kroemer G, Billiar TR, Van Houten B, Zeh HJ 3rd, Lotze MT. High-mobility group box 1 is essential for mitochondrial quality control. Cell Metab/. 2011; 13(6): 701–711.
53. King M, Nafar F, Clarke J, Mearow K. The small heat shock protein Hsp27 protects cortical neurons against the toxic effects of beta-amyloid peptide. J. Neurosci. Res. 2009; 87(14):3161–3175. [PubMed: 19530165]
54. Samali A, Robertson JD, Peterson E, Manero F, van Zeijl L, Paul C, Cotgreave IA, Arrigo AP, Orrenius S. Hsp27 protects mitochondria of thermotolerant cells against apoptotic stimuli. Cell Stress Chaperones. 2001; 6(1):49–58. [PubMed: 11525243]
55. Danton GH, Dietrich WD. Inflammatory mechanisms after ischemia and stroke. J. Neuropath. Exp. Neurol. 2003; 62(2):127–136. [PubMed: 12578222]
56. Stoll G, Jander S, Schroeter M. Detrimental and beneficial effects of injury-induced inflammation and cytokine expression in the nervous system. Adv. Exp. Med. Biol. 2002; 513:87–113. [PubMed: 12575818]
57. Stamatovic SM, Shakui P, Keep RF, Moore BB, Kunkel SL, Van Rooijen N, Andjelkovic AV. Monocyte chemoattractant protein-1 regulation of blood-brain barrier permeability. J. Cereb. Blood Flow Metab. 2005; 25(5):593–606. [PubMed: 15689955]
58. Lu TS, Chen HW, Huang MH, Wang SJ, Yang RC. Heat shock treatment protects osmotic stress-induced dysfunction of the blood-brain barrier through preservation of tight junction proteins. Cell Stress Chaperones. 2004; 9(4):369–377. [PubMed: 15633295]
59. Kato H, Kogure K, Liu XH, Araki T, Kato K, Itoyama Y. Immunohistochemical localization of the low molecular weight stress protein HSP27 following focal cerebral ischemia in the rat. Brain Res. Brain Re.s Protoc. 1995; 679(1):1–7.
60. Nishino K, Nowak TS Jr. Time course and cellular distribution of hsp27 and hsp72 stress protein expression in a quantitative gerbil model of ischemic injury and tolerance: thresholds for hsp72 induction and hilar lesioning in the context of ischemic preconditioning. J. Cereb. Blood Flow Metab. 2004; 24(2):167–178. [PubMed: 14747743]

61. Currie RW, Ellison JA, White RF, Feuerstein GZ, Wang X, Barone FC. Benign focal ischemic preconditioning induces neuronal Hsp70 and prolonged astrogliosis with expression of Hsp27. Brain Res. Brain Re.s Protoc. 2000; 863(1-2):169–181.

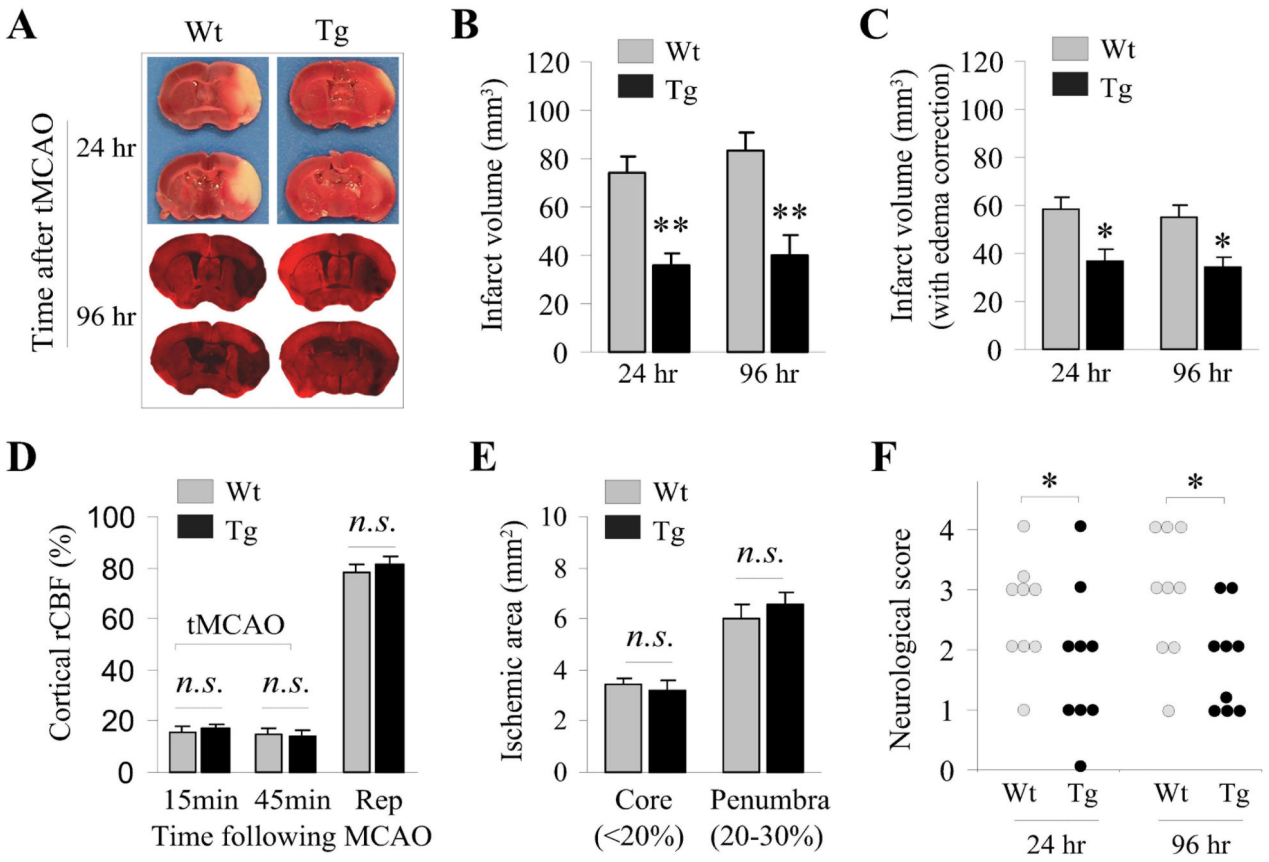

Figure 1. HSP27 reduces infarct volume and behavioral deficits following ischemic injury

A: TTC staining at 24 h and MAP2 staining at 96 h following transient middle cerebral artery occlusion (tMCAO) in HSP27 overexpressing transgenics (Tg) versus wild-type animals (Wt). Two rostrocaudal levels through the striatum and cortex are illustrated for each stain. **B**: Infarct volumes were estimated by summing the area of loss of TTC staining at 24 h after tMCAO and the area of loss of MAP2 staining at 96 h after tMCAO. N = 9 mice / group. **C**: The volume of the infarct was also indirectly measured by measuring the MAP2 and TTC-positive region in the ipsilateral hemisphere and subtracting it from the size of the contralateral hemisphere. This reduces the impact of brain swelling and edema on infarct volume measurements by only measuring relatively healthy, non-edematous tissue. Infarct volumes as measured directly and indirectly in B and C were significantly reduced in transgenics. N = 9 mice / group. **D**: Regional cerebral blood blow (rCBF) in the cortex was measured by laser Doppler 15 min and 45 min following initiation of tMCAO and 15 min into reperfusion (Rep). rCBF was not impacted by transgene expression. N = 6 mice / group. *n.s.* implies no significant difference. **E**: Ischemic area was measured by laser speckle and was not affected by transgene expression in either the core (0-20% residual CBF) or the penumbra (20-30% residual CBF) of the infarct. N = 6 mice / group. **F**: Neurological scores were evaluated as deficits in behavior (greater score = higher deficits). Scores were reduced in transgenics at both 24 h and 96 h following tMCAO. N = 9 mice / group. * $p \leq 0.05$ or ** $p \leq 0.01$ for comparison of HSP27 transgenics *versus* wild-type animals.

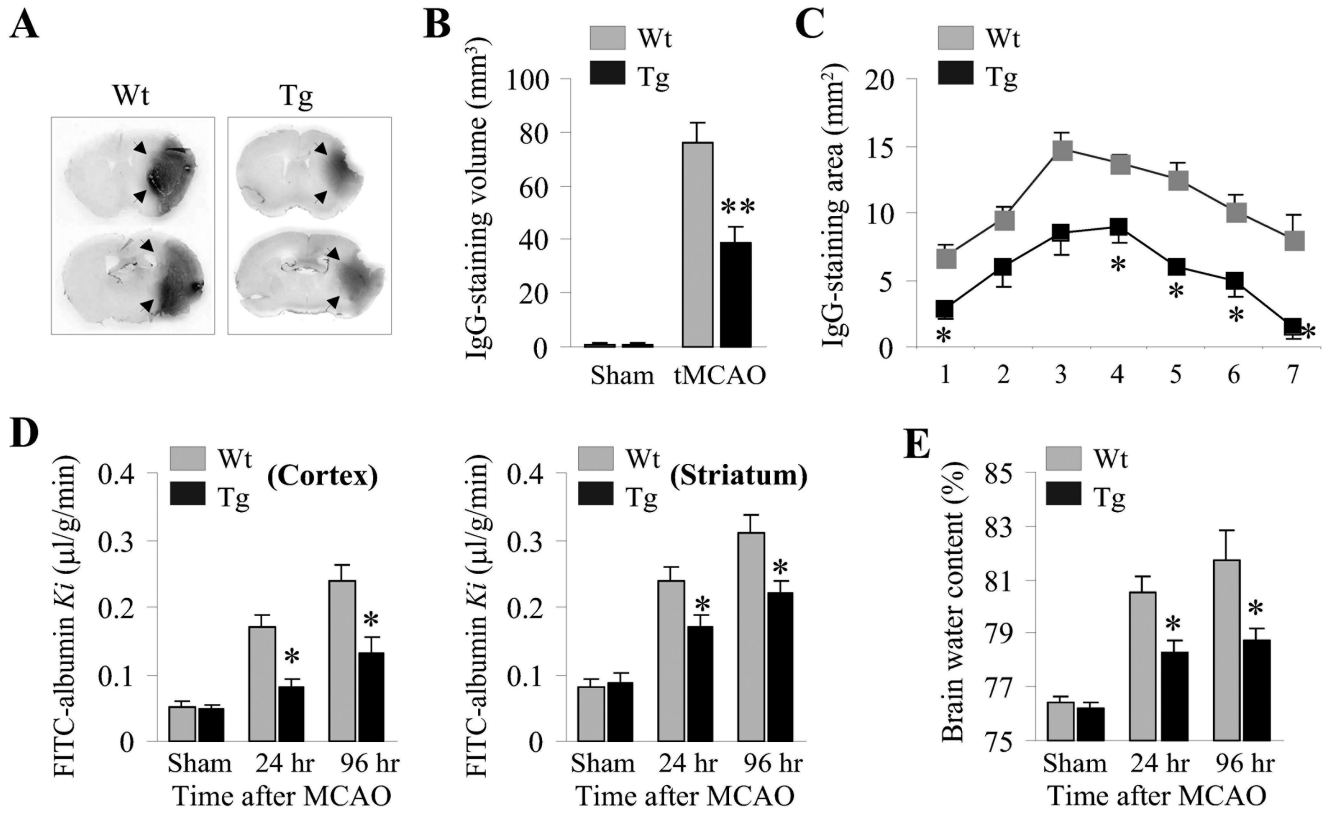

Figure 2. HSP27 protects against the rise in BBB permeability following ischemia

A: Endogenous IgG extravasation into the parenchyma was visualized by staining sections with antibodies against mouse IgG molecules. Two rostrocaudal levels are shown through the striatum and overlying cortex. Arrowheads indicate the boundaries of the stain. **B**: Measurements of the volume of IgG staining in sham wild-type and transgenic animals or animals subjected to tMCAO. Transgene expression reduced the volume of the IgG staining region following tMCAO. N = 6 mice / group. **C**: The rostrocaudal extent of the area of IgG staining is shown for 7 coronal sections per animal. The numbers on the X-axis each delineate 1 out of the 7 coronal sections from rostral (section 1) to caudal (section 7). The sections span the affected region at 1 mm intervals. Protection was evident across almost the full rostrocaudal extent of the BBB lesion. N = 6 mice / group. **D**: Extravasation of exogenous FITC-albumin into cortical and striatal parenchyma (expressed as the blood-brain transfer coefficient *K*i) reveals that HSP27 overexpression reduced loss of BBB integrity following tMCAO. N = 6-7 mice / group. **E**: HSP27 overexpression also protected against water entry into brain parenchyma following tMCAO. N = 5 Wt and 7 Tg mice. * $p \leq 0.05$ or ** $p \leq 0.01$ for transgenic *versus* wild-type animals.

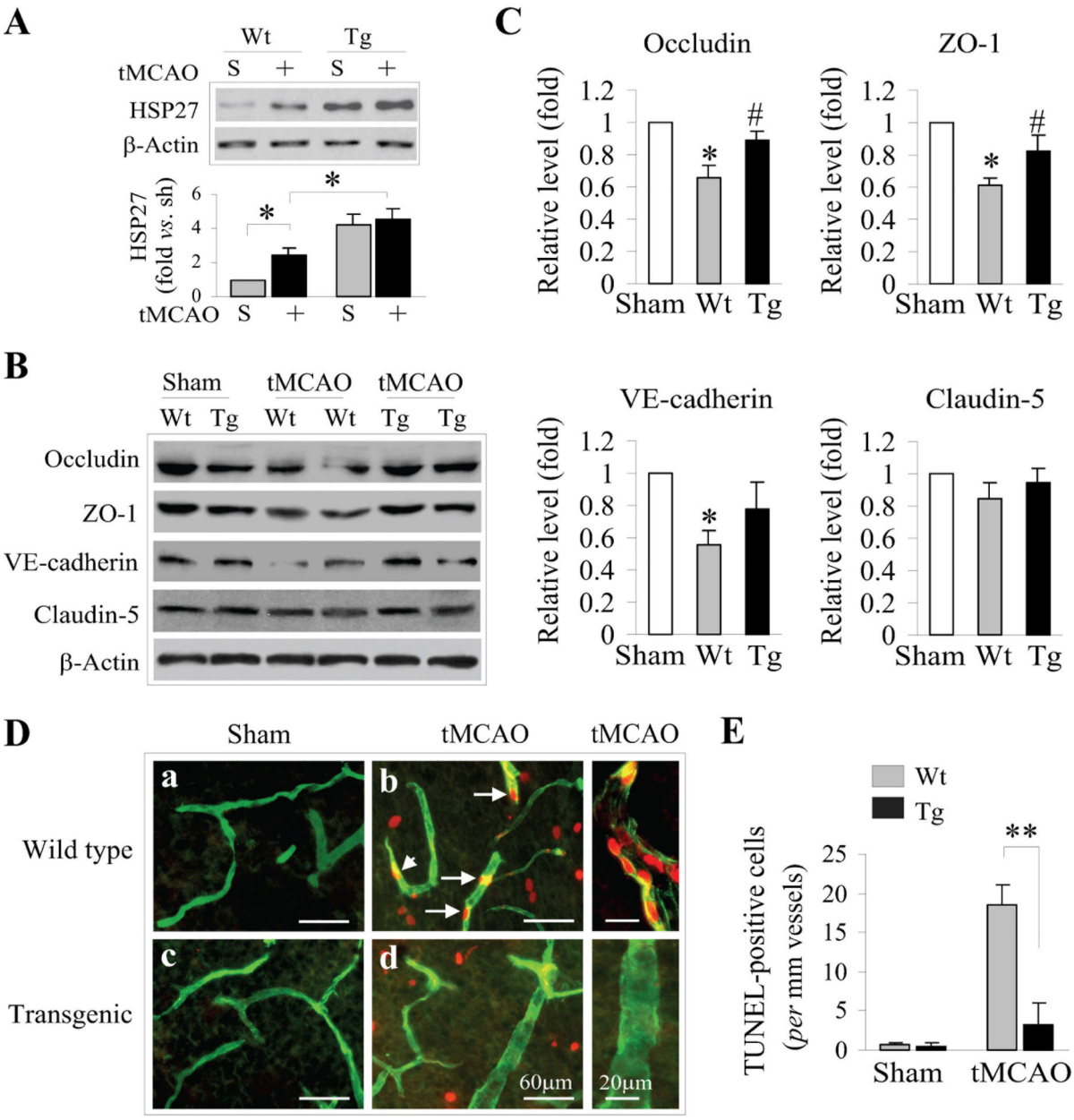

Figure 3. HSP27 reduces loss of microvessel proteins and apoptosis in microvessel walls

A: Microvessels were isolated by their preferential adherence to glass beads. HSP27 was induced by tMCAO in wild-type animals in microvessel lysates. High basal expression of HSP27 in transgenics precluded a large rise in HSP27 following tMCAO. Transgenics exhibited higher expression of HSP27 under tMCAO conditions than wild-type animals. S denotes sham surgeries, + denotes tMCAO. N = 3 mice / group. * $p \leq 0.05$ for indicated comparisons. **B**: Western immunoblots of microvessel proteins occludin, ZO-1, VE-cadherin, and claudin-5 reveal loss in all but claudin-5 with tMCAO. This effect was lessened in transgenics, as is evident from the quantification in **C**. N = 5-6 mice / group. * $p \leq 0.05$ for statistical comparison of Wt *versus* sham animals; # $p \leq 0.05$ Wt *versus* transgenics. **D**: Dual immunofluorescence for a microvessel-staining lectin (green) and

TUNEL staining (red) in the cerebral cortex reveals apoptotic profiles along microvessel walls and within brain parenchyma following tMCAO. TUNEL positive cells along microvessels are quantified in **E**. HSP27 overexpression protected against apoptosis in microvessel walls following tMCAO. N = 5 mice / group. ** $p \leq 0.01$ for transgenic *versus* wild-type animals.

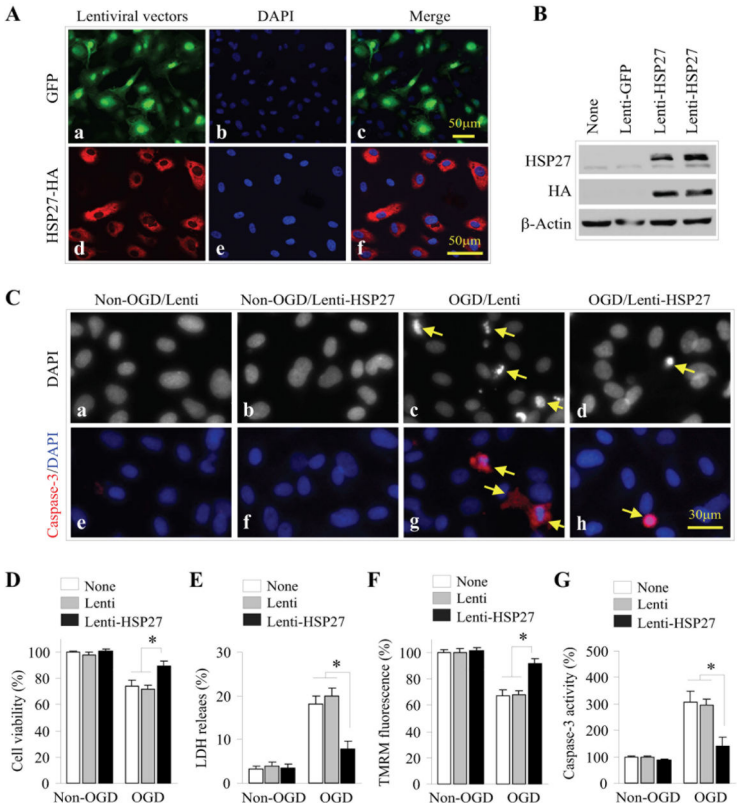

Figure 4. Lentivirus-mediated HSP27 overexpressison in primary endothelial cell cultures protects against oxygen-glucose deprivation (OGD)

A: Infection of primary endothelial cells by a lenti-GFP (a-c) and a lenti-HSP27-HA (d-f) construct reveals expression of GFP (green) or the HA tag (red) in DAPI stained (blue) cells. **B**: Western immunoblotting for HSP27 and the HA construct in primary endothelial cells that were sham-infected or infected with lentiviral particles bearing GFP or the HSP27 gene. HSP27 and HA were only expressed in cultures infected with lenti-HSP27. **C**: DAPI nuclear staining (a-d) and immunostaining for active (cleaved) caspase 3 (e-h) reveal that endothelial cultures infected with lenti-HSP27 exhibited fewer condensed and fragmented nuclei and expressed less activated caspase 3 protein than control cultures subjected to OGD. **D**: MTT assay for mitochondrial activity in control cultures or cultures exposed to OGD following sham infection or infection with control lentiviral particles or lenti-HSP27. HSP27 infection protected endothelial cells from loss of viability in response to OGD. **E**: LDH release from endothelial cells through damaged membranes following OGD was also reduced by lenti-HSP27. **F**: HSP27 overexpression in endothelial cells protected against loss of mitochondrial membrane potential (loss of TMRM fluorescence) following OGD. **G**: As expected from the immunofluorescence data in C, lentiviral HSP27 infection reduced the rise in caspase 3 activity following OGD in endothelial cells. N = 3-4 independent experiments. * $p \leq 0.05$ for comparison of lenti-HSP27 *versus* both sham infections and control lentivirus infections.

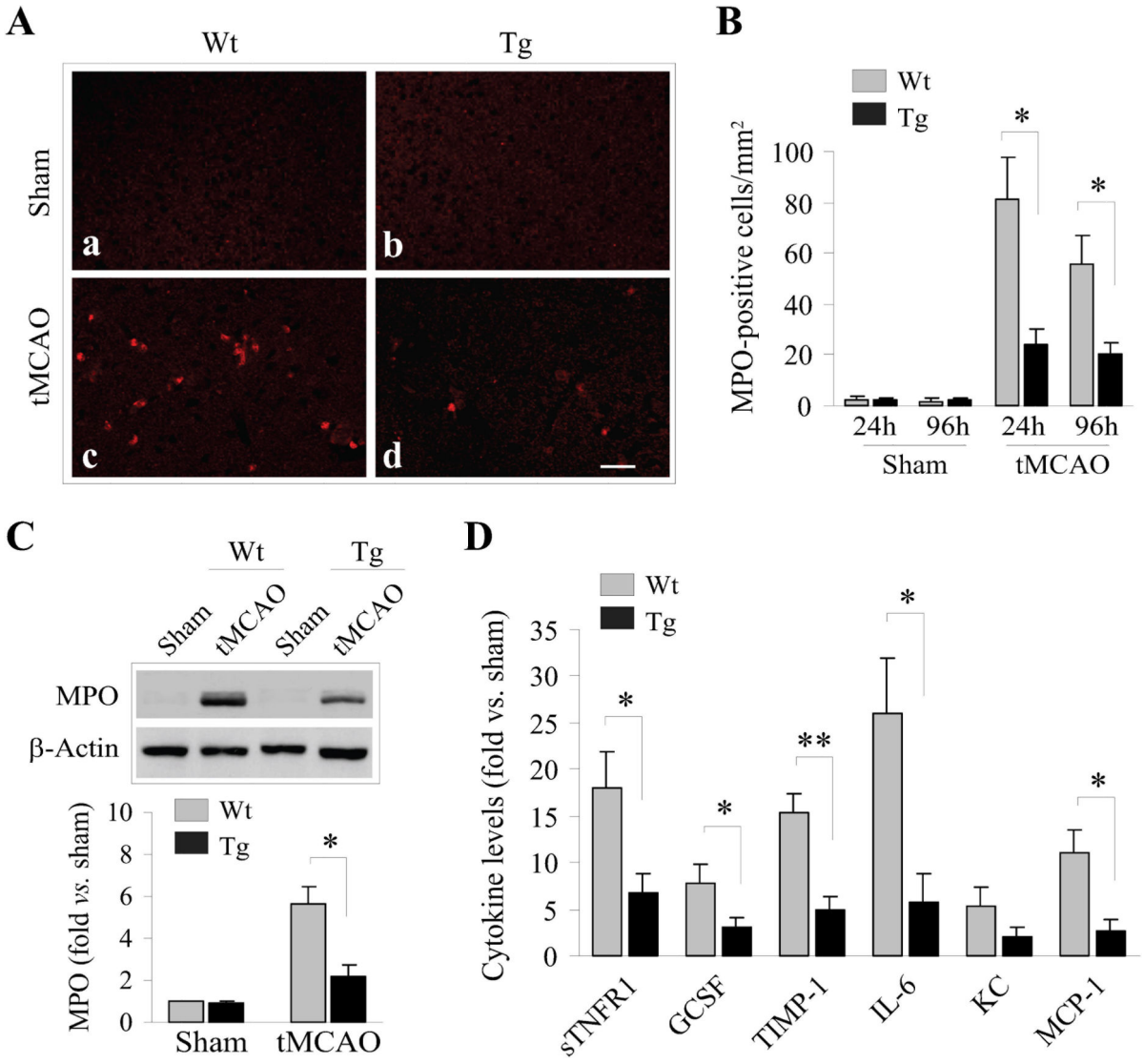

Figure 5. HSP27 overexpression protects against brain neutrophil invasion and cytokine release 24 h following tMCAO

A: Immunofluorescent staining for MPO-positive neutrophils in the cortex reveals increased invasion by blood-borne cells in wild-type animals following tMCAO. Scale bar denotes 30 μm. Numbers of MPO-positive cells are quantified in **B** and show that HSP27 overexpression protected against the rise in these MPO-positive profiles. N = 5-6 mice / group. **C**: Western immunoblotting for cortical MPO protein levels confirms data in B as there was a reduction in MPO protein in transgenics following tMCAO. N = 4 mice / group. **D**: Fold increases in cytokine release following tMCAO illustrate the reduction in inflammatory markers in transgenics. Thirty-two cytokines were measured by protein array. Shown are levels of soluble tumor necrosis factor receptor 1 (sTFNR1), granulocyte colony stimulating factor (GCSF), tissue inhibitor of metalloproteinases 1 (TIMP1), interleukin-6 (IL-6), monocyte chemoattractant protein 1 (MCP-1) and the protein KC (melanoma

growth-stimulating activity gene). N = 3 mice / group. * $p \leq 0.05$ or ** $p \leq 0.01$ for transgenic *versus* wild-type animals.